Measurement of Short-Range Correlations in Radioactive Nuclei using Inverse Kinematics

Hang Qi | 06 / 2026

SRC Pair Formation in Neutron-Rich Nuclei

- M. Duer (e,e'p) result:
  - SRC pair formation correlated with N/Z asymmetry
- Recent CaFe result:
  - SRC pair formation impacted by quantum structure of the nucleus

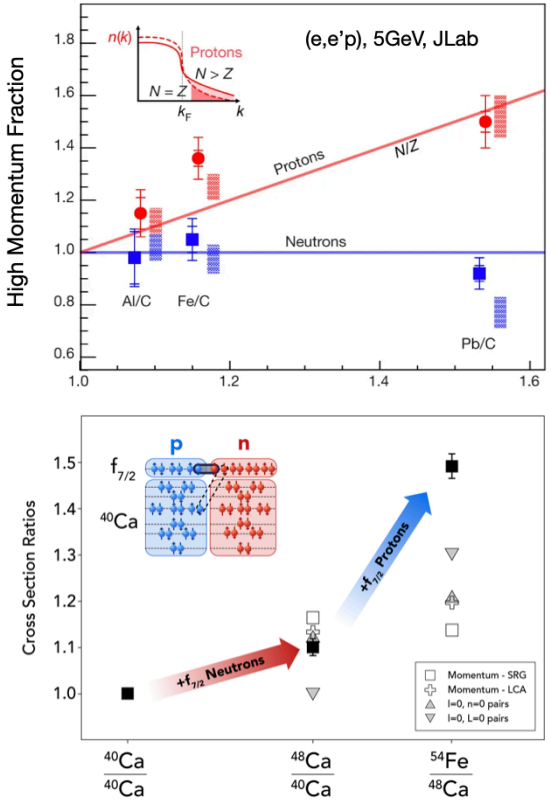

M. Duer et al. (CLAS), Nature 2018 · E. W. Wertz et al. (CaFe Collaboration), Nature (2026)

SRC Pair Formation in Neutron-Rich Nuclei

- M. Duer (e,e'p) result:
  - SRC pair formation correlated with N/Z asymmetry
- Recent CaFe result:
  - SRC pair formation impacted by quantum structure of the nucleus

- SRC study along isotopic chain
  - Separate mass vs. nuclear structure effects
  - Radioactive isotopes provide large asymmetry

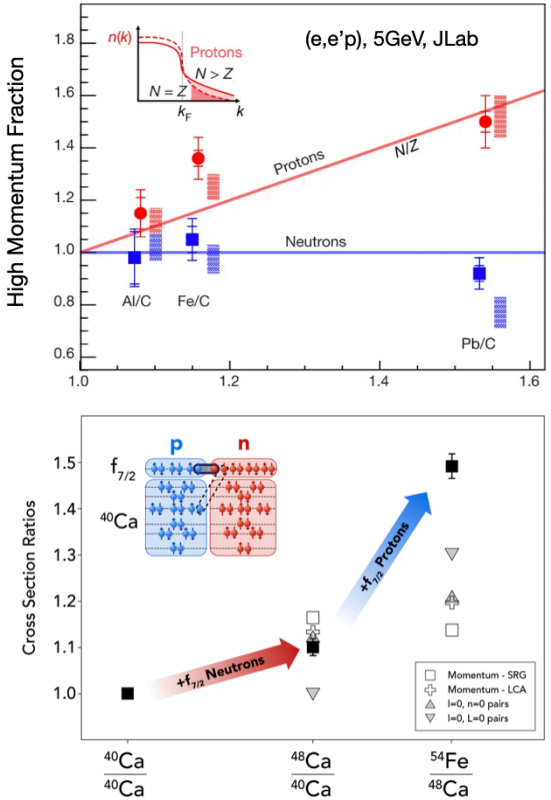

M. Duer et al. (CLAS), Nature 2018 · E. W. Wertz et al. (CaFe Collaboration), Nature (2026)

A New Method to Study SRC

Proton Probe + Inverse Kinematics

Previous Work (Patsyuk et al., Nat. Phys. 2021)

- Only method to access extremely neutron-rich, unstable nuclei
- Hadronic probe study on ^{12}C
  - Limited statistics
  - 3.2 GeV/u beam energy

This Study

- Significant statistics of SRC in ^{12}C
- First SRC signal in radioactive nuclei ^{16}C

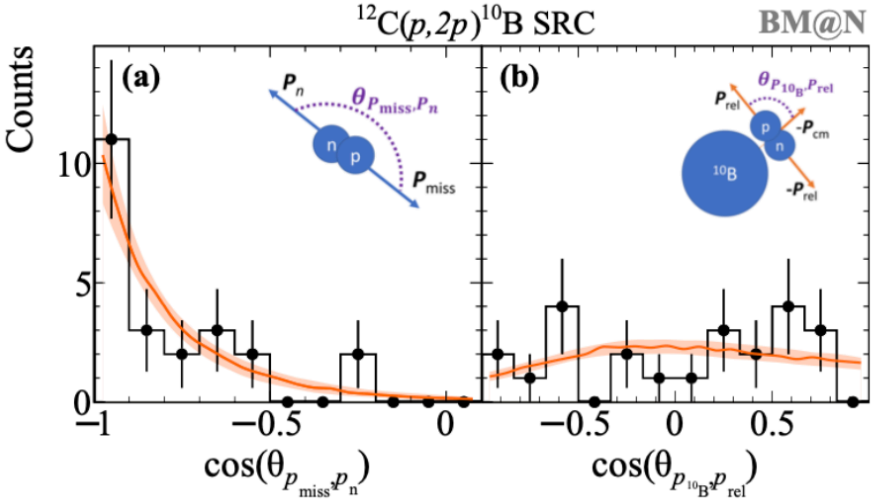

Patsyuk et al., Nat. Phys. 2021

A New Method to Study SRC: Proton Probe + Inverse Kinematics

SRC with significant statistics in ^{12}C

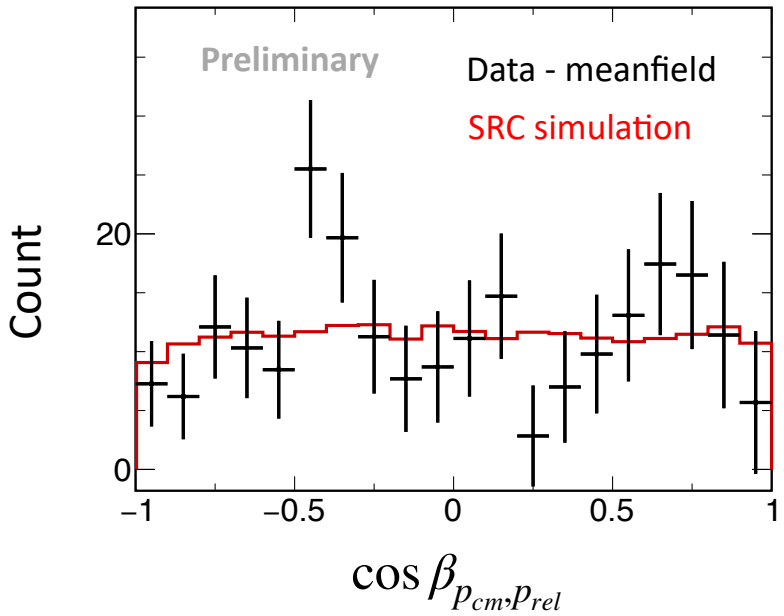

First SRC signal in ^{16}C

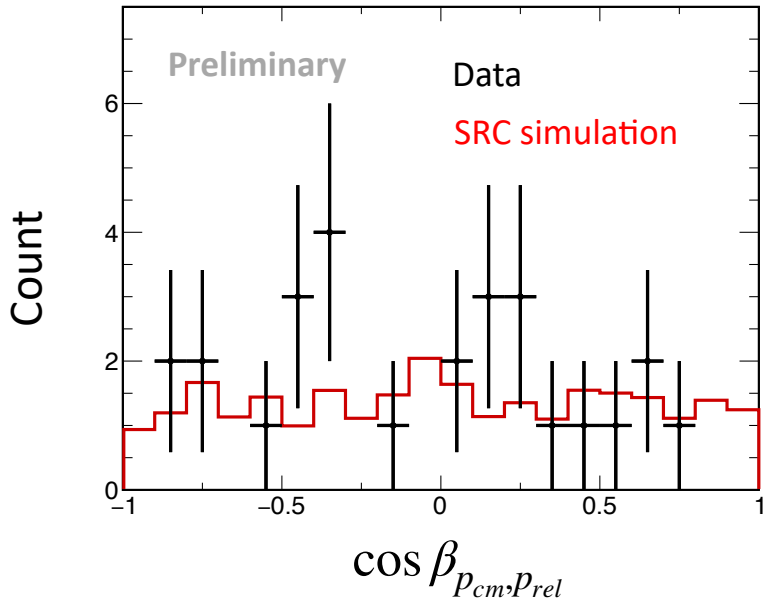

Exclusive SRC Measurement with Inverse Kinematics

- Beam nucleus strikes liquid hydrogen target proton
- Two knockout protons detected
- A–2 fragment identified downstream
- Recoil nucleon reconstructed from kinematics

Key Kinematic Relations

- $p_{rec} = p_{beam} + p_{tg} - p_1 - p_2 - p_{A-2}$
- $p_{miss} = p_1 + p_2 - p_{tg}$
- $\alpha_{miss} = (E_{miss} - P_{miss,z}) / m_N$

$^{12}C(p,2p)^{10}B$ reaction

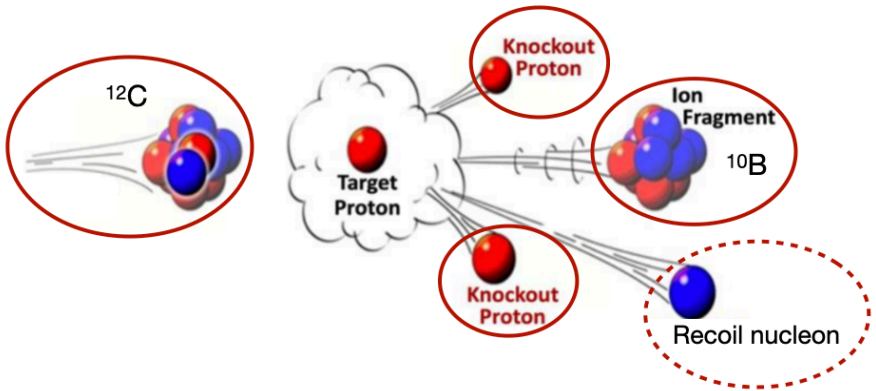

Quasi-Free Reaction Selections

Suppression of ISI/FSI Effects

Reaction Channels

- (p,2p) event selection
- A–2 fragment identification
  - pn-SRC in ^{12}C: ^{12}C(p,2p)^{10}B
  - pn-SRC in ^{12}C: ^{12}C(p,2p)^{10}Be
  - pn-SRC in ^{16}C: ^{16}C(p,2p)^{14}B
  - pp-SRC in ^{16}C: ^{16}C(p,2p)^{14}Be
  - pn-SRC in ^{16}C: ^{16}C(p,2p)^{14}B*→^{13}B+n

Beam Energy

1.25 GeV/u

Intensity

1×10^5 pps

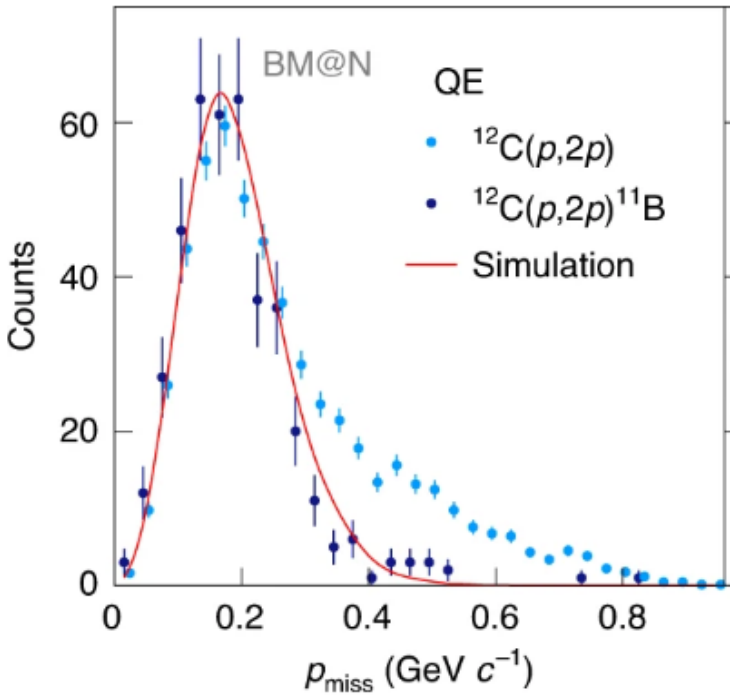

Patsyuk et al., Nat. Phys. 2021

Quasi-Free Reaction Selections

Suppression of ISI/FSI Effects

Reaction Channels

- (p,2p) event selection
- A–2 fragment identification
  - pn-SRC in ^{12}C: ^{12}C(p,2p)^{10}B
  - pn-SRC in ^{12}C: ^{12}C(p,2p)^{10}Be
  - pn-SRC in ^{16}C: ^{16}C(p,2p)^{14}B
  - pp-SRC in ^{16}C: ^{16}C(p,2p)^{14}Be
  - pn-SRC in ^{16}C: ^{16}C(p,2p)^{14}B*→^{13}B+n

Beam Energy

1.25 GeV/u

Intensity

1×10^5 pps

Fragment Identification in ^{12}C(p,2p) reaction

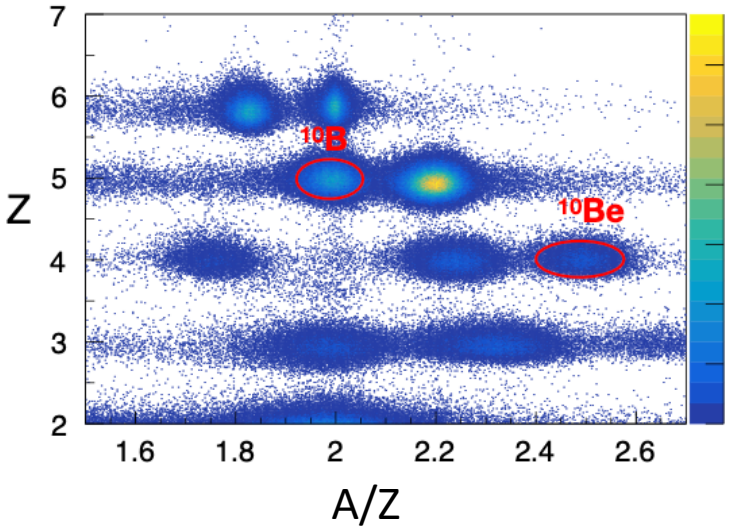

Quasi-Free Reaction Selections

Suppression of ISI/FSI Effects

Reaction Channels

- (p,2p) + A–2 fragment selection
- All five channels: $^{12}C \rightarrow {}^{10}B$, $^{12}C \rightarrow {}^{10}Be$, $^{16}C \rightarrow {}^{14}B$, $^{16}C \rightarrow {}^{14}Be$, $^{16}C \rightarrow {}^{13}B+n$

Kinematic Cuts

- $|t|, |u| > 0.8$ GeV²
- $0.3 < M^2_{miss} < 1.5$ GeV²/c⁴

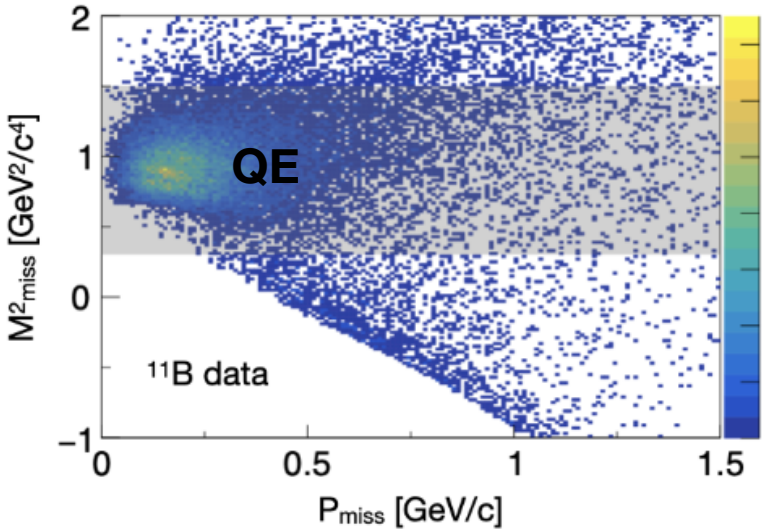

GCF Simulation for SRC Description

GCF describes SRC pairs across nuclei in electron scatterings

Generalized Contact Formalism (GCF)

- Universal description of SRC pairs across different nuclei electron-scattering data
- Two-body contact encodes short-distance nuclear structure; relative wavefunction from NN potential (AV18/AV4')

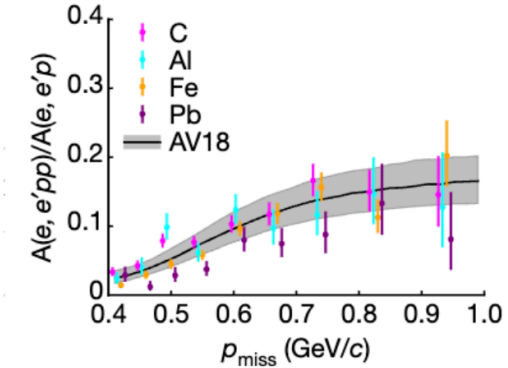

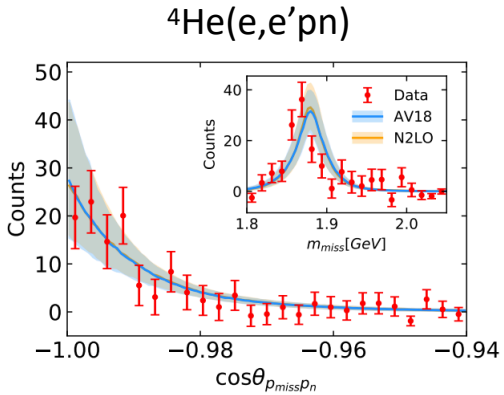

A. Schmidt et al. (CLAS), Nature 578, 540–544 (2020) · *J. R. Pybus et al., Phys. Lett. B 805, 135429 (2020)*

pn-SRC Identification in ^{12}C

Kinematic distributions after preliminary SRC selections

Mean-field simulation needed to describe tail region

Selections

- (p,2p) tagging
- ^{10}B fragment tagging
- $|t|,|u| > 0.8$ GeV²
- $0.3 < M^2_{miss} < 1.5$ GeV²/c⁴
- $p_{miss} > 0.4$ GeV/c

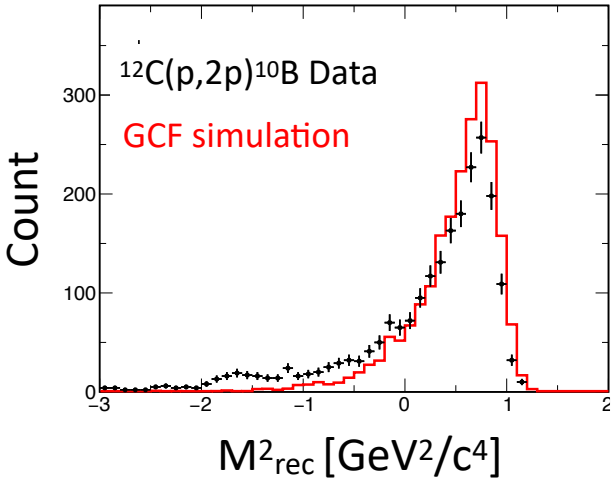

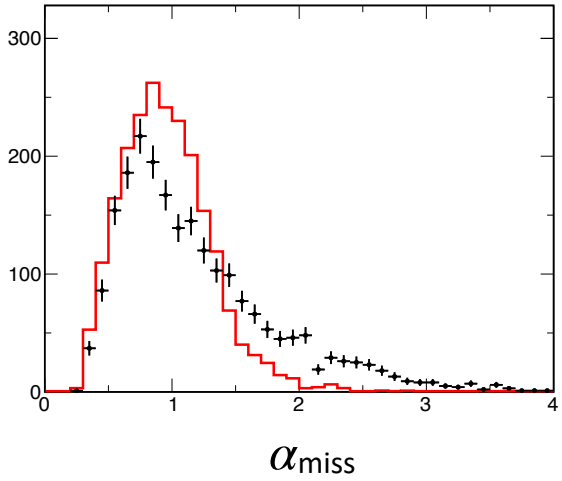

pn-SRC Identification in ^{12}C

Simulation guided SRC selection

- INCL (intra-nuclear cascade model)
- Mean-field nucleon evaporation: $^{12}C(p,2p)^{11}B^{*}\rightarrow^{10}B + n$
- Multiple re-scattering of final state particles

Selections

- (p,2p) tagging
- ^{10}B fragment tagging
- $|t|,|u| > 0.8$ GeV²
- $0.3 < M^2_{miss} < 1.5$ GeV²/c⁴
- $p_{miss} > 0.4$ GeV/c

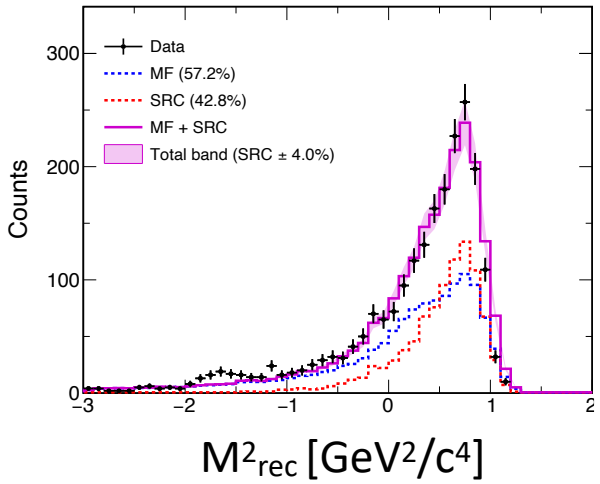

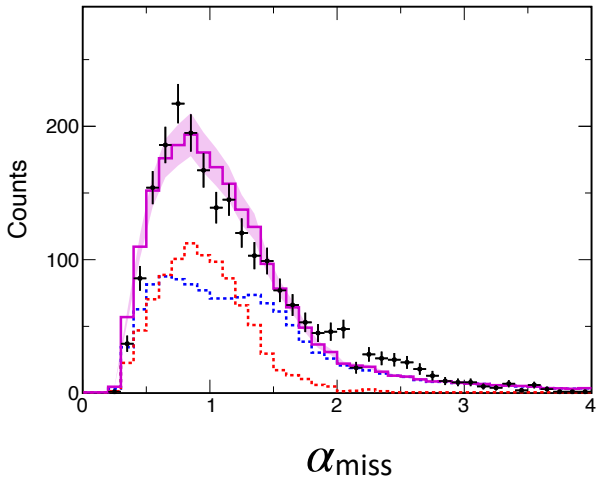

pn-SRC Identification in ^{12}C

Simulation guided SRC selection

- INCL (intra-nuclear cascade model)
- Mean-field nucleon evaporation: $^{12}C(p,2p)^{11}B^{*}\rightarrow^{10}B + n$
- Multiple re-scattering of final state particles

Selections

- (p,2p) tagging
- ^{10}B fragment tagging
- $|t|,|u| > 0.8$ GeV²
- $0.3 < M^2_{miss} < 1.5$ GeV²/c⁴
- $p_{miss} > 0.4$ GeV/c
- **+ $\alpha_{miss} < 1.2$**

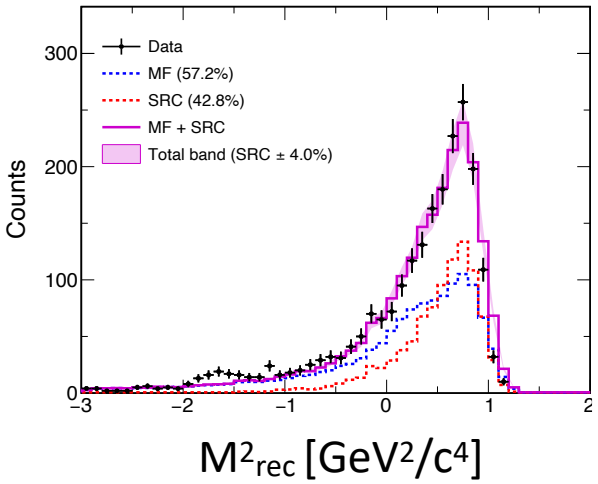

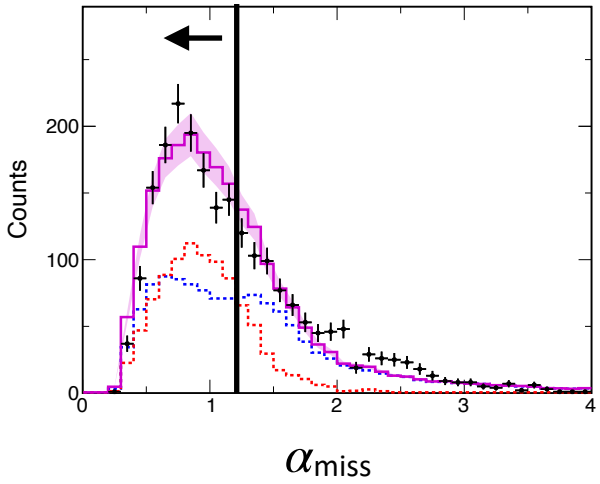

Experimental Signature for SRC Factorization

Back-to-back nucleon pair

- Large relative momentum p_rel
- Low pair center-of-mass momentum
- Knocked-out proton momentum back-to-back with recoil nucleon
- Expected signature:

  $\cos \alpha_{pmiss,prec} \sim -1$

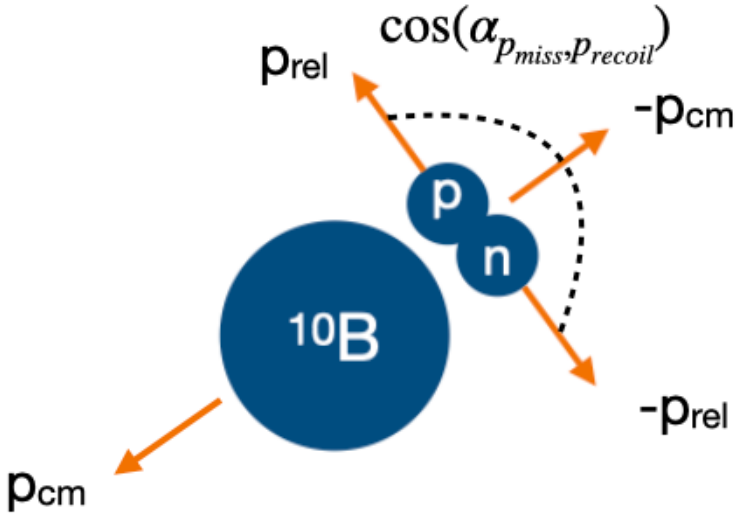

Back-to-Back SRC Pair in ^{12}C

SRC universality

Consistent back-to-back nucleon pair signal in electron and proton scatterings

- $|t|,|u| > 0.8$ GeV²
- A-2 fragment selection
- $0.3 < M^2\_miss < 1.5$ GeV²/c⁴
- p_miss > 0.4 GeV/c
- α_miss < 1.2

$^{12}C(e,e'p)$

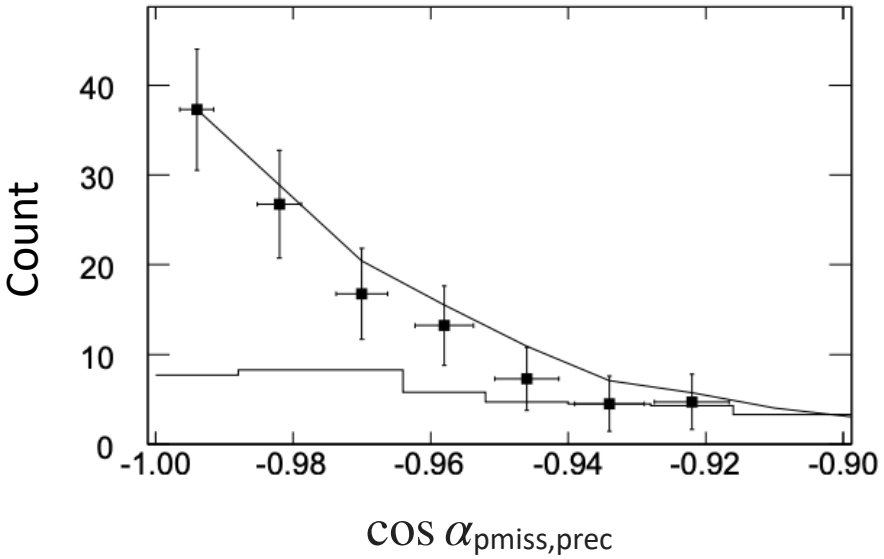

pn-SRC: $^{12}C(p,2p)^{10}B$

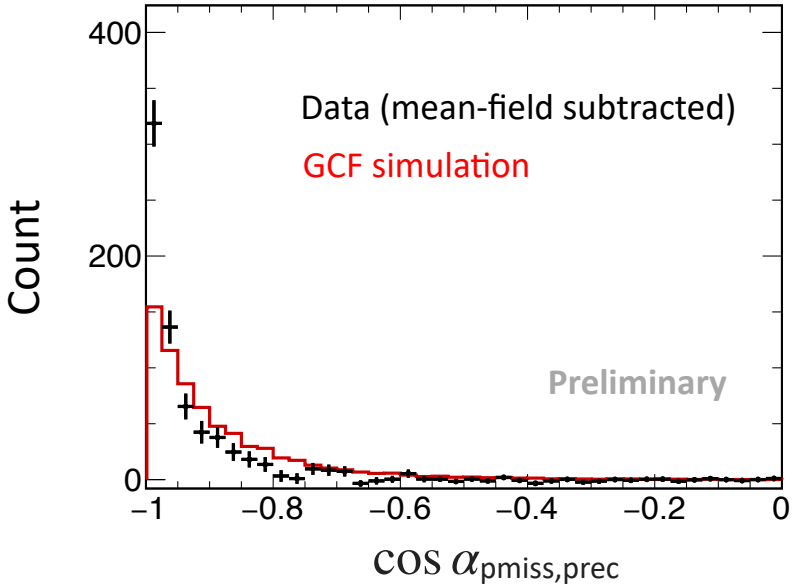

R. Shneor et al., Phys. Rev. Lett. 99, 072501 (2007)

Back-to-Back SRC Pair in ^{12}C

SRC universality

Back-to-back nucleon pair signal for both pp- and pn-SRC pairs in ^{12}C in proton scattering

- $|t|,|u| > 0.8$ GeV²
- A-2 fragment selection
- $0.3 < M^2\_miss < 1.5$ GeV²/c⁴
- p_miss > 0.4 GeV/c
- α_miss < 1.2

pn-SRC: $^{12}C(p,2p)^{10}B$

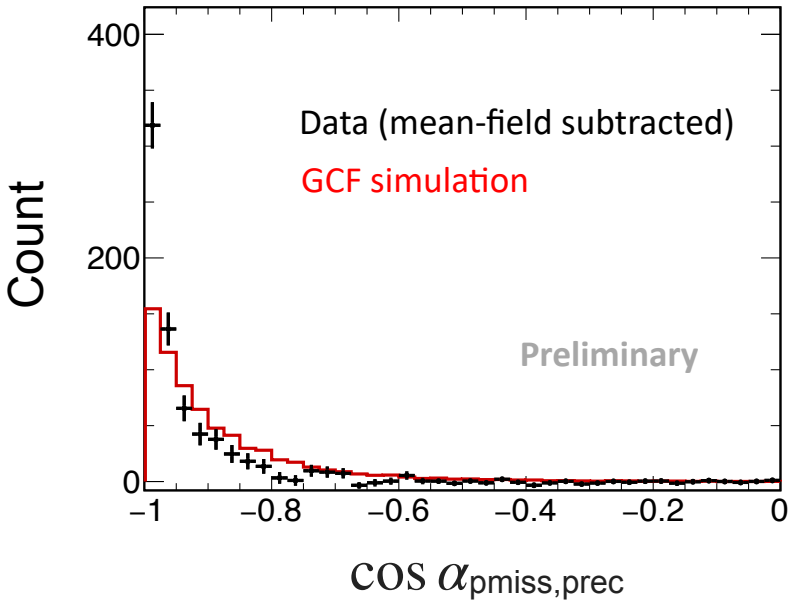

pp-SRC: $^{12}C(p,2p)^{10}Be$

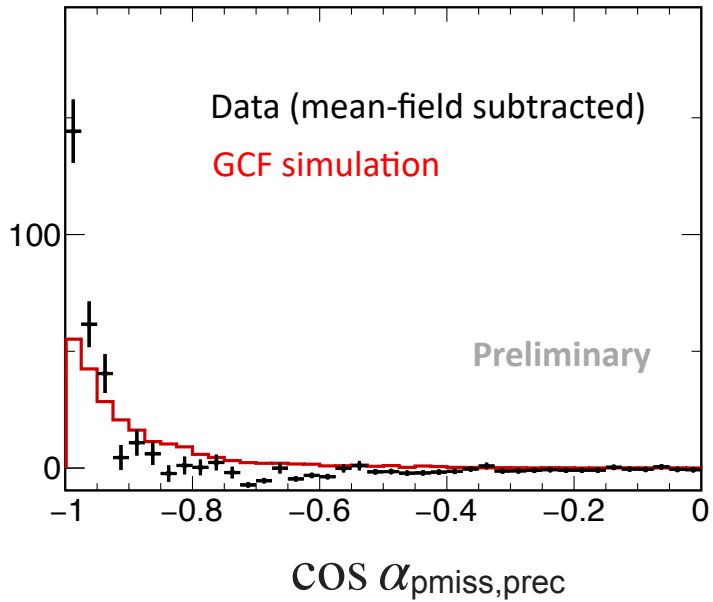

SRC Factorization

No correlation between relative & c.m. motion

GCF Factorization Ansatz

- $f(p_{rel}, p_{cm}) \approx C(p_{cm}) \times \varphi(p_{rel})$

- p_{rel} and p_{cm} are uncorrelated in SRC pairs
- Measurable as angular decorrelation

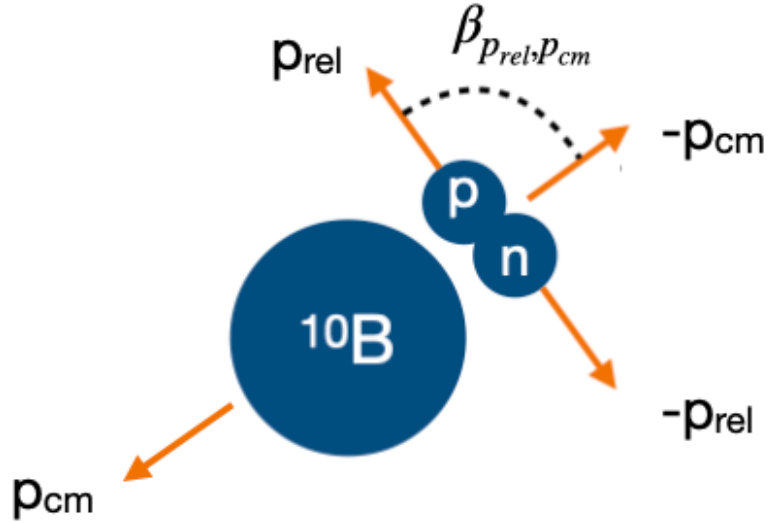

SRC Factorization in ^{12}C

- $|t|,|u| > 0.8$ GeV²
- A-2 fragment selection
- $0.3 < M^2\_miss < 1.5$ GeV²/c⁴
- p_miss > 0.4 GeV/c
- α_miss < 1.2

pn-SRC: $^{12}C(p,2p)^{10}B$

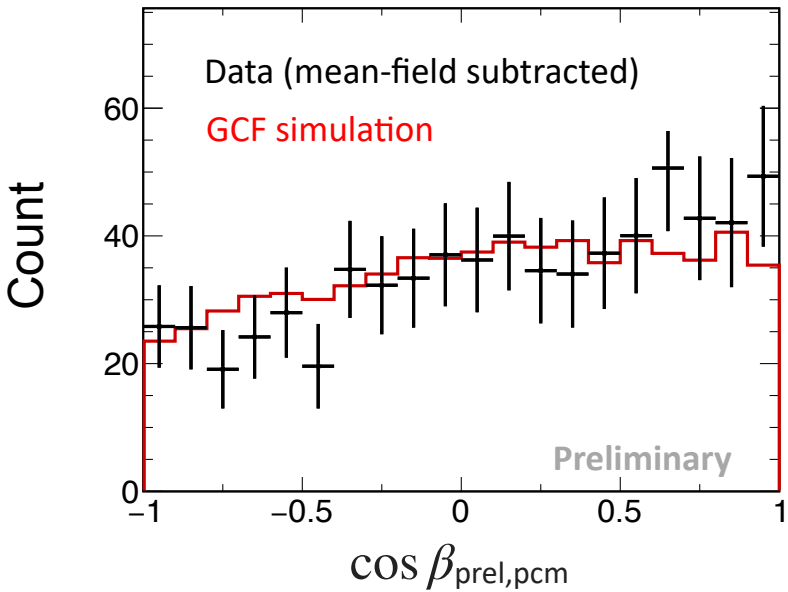

pp-SRC: $^{12}C(p,2p)^{10}Be$

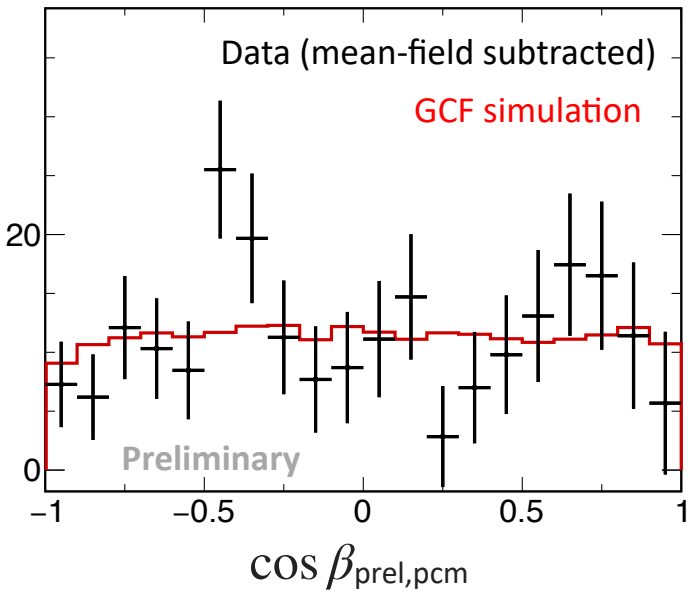

SRC pn/pp Ratio in ^{12}C

pn-SRC yield | $^{12}C(p,2p)^{10}B$

687 ± 54

SRC fraction: 51.8 ± 4.1%

pp-SRC yield | $^{12}C(p,2p)^{10}Be$

227 ± 36

SRC fraction: 44.8 ± 7.1%

Observed pn/pp ratio (^{10}B / ^{10}Be channels)

3.0 ± 0.5

Expected integrated pn/pp ratio

~ 10.4 ± 0.2

Single-charge exchange (SCE 2% - 8%) accounts for only a fraction of the suppression.
Final-state selectivity is the dominant effect on the observed pn/pp ratio.

NN Potential Discrimination

Through pn-SRC data in ^{12}C

- SRC wavefunction encodes the NN potential
- AV18 (full realistic) vs AV4' (simplified)
- Pn channel (s=1): NN potential discrimination

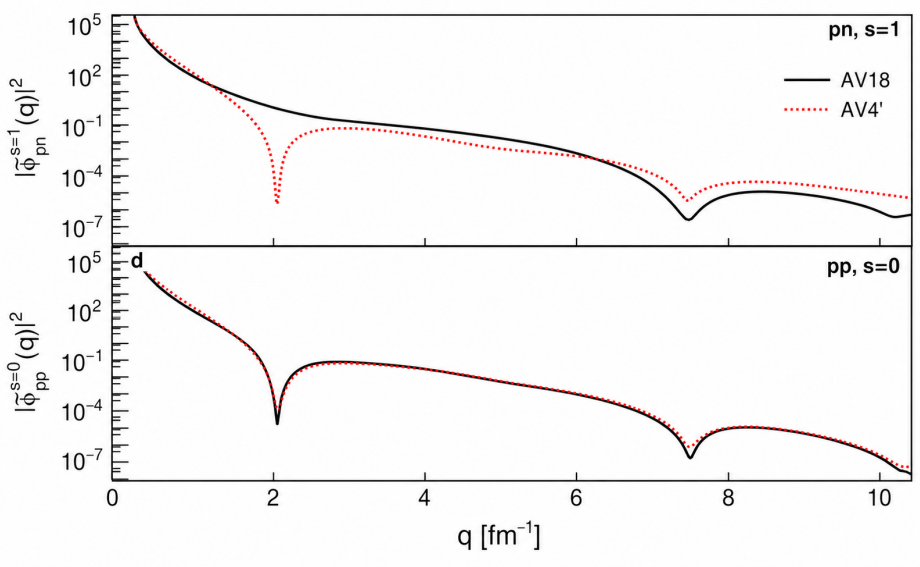

SRC Data in ^{12}C Favors Realistic AV18 Potential over AV4'

$|t|,|u| > 0.8$ GeV²
A-2 fragment selection
$0.3 < M^2\_miss < 1.5$ GeV²/c⁴
p_miss > 0.4 GeV/c

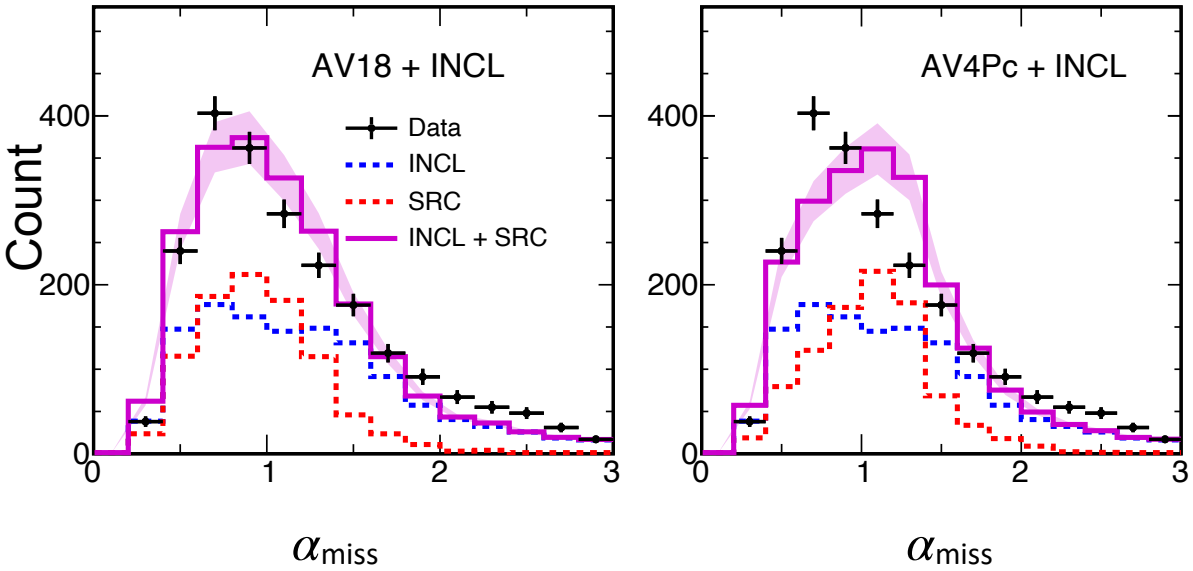

SRC Data in ^{12}C Favors Realistic AV18 Potential over AV4'

$|t|,|u| > 0.8$ GeV²
A-2 fragment selection
$0.3 < M^2\_miss < 1.5$ GeV²/c⁴
p_miss > 0.4 GeV/c

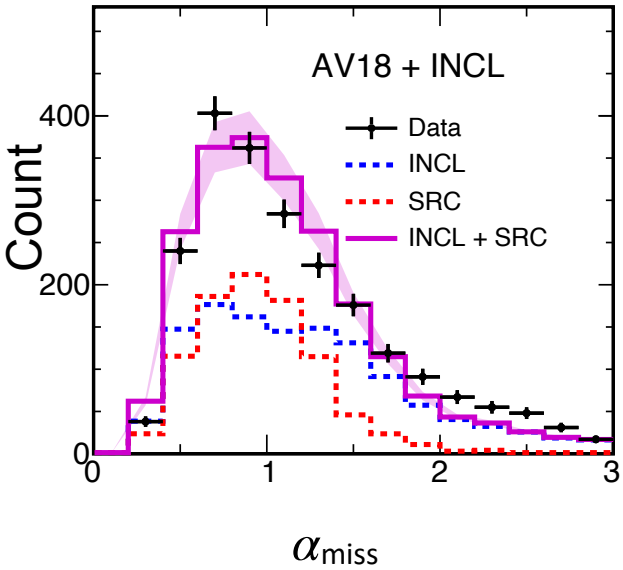

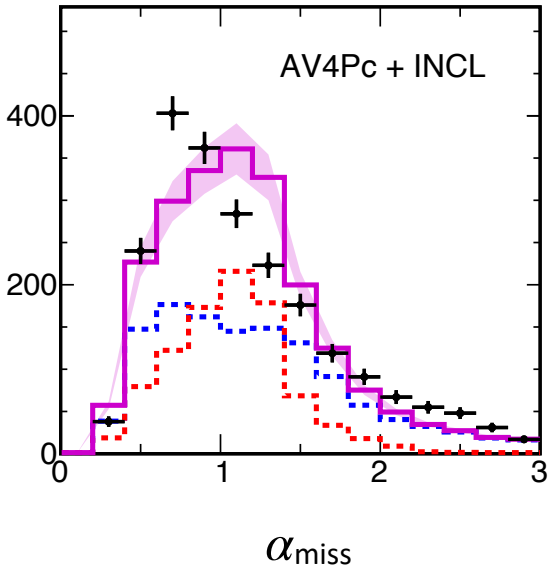

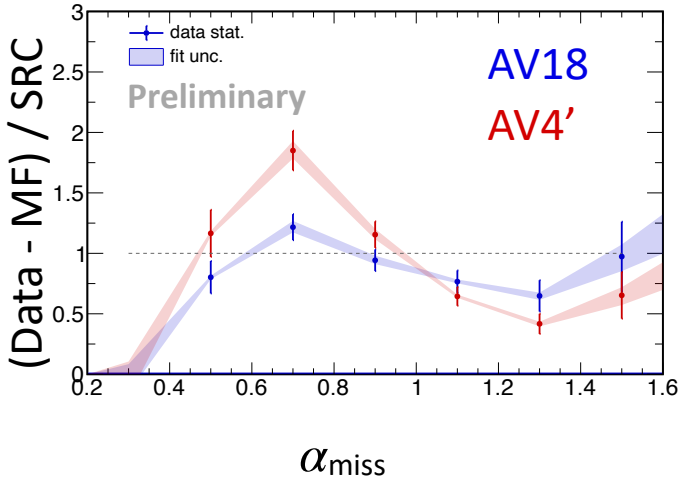

From ^{12}C to ^{16}C

Established: SRC in ^{12}C with Proton Probes + Inverse Kinematics

- SRC identified with significant statistics
- SRC signatures consistent with electron-scattering results
- NN potential discrimination using SRC data

First Search: SRC in Radioactive ^{16}C Nucleus

- pn-SRC: $^{16}C(p,2p)^{14}B$ and $^{16}C(p,2p)^{14}B^* \rightarrow ^{13}B+n$
- pp-SRC: $^{16}C(p,2p)^{14}Be$

Fragment Identification in $^{16}C(p,2p)$ reaction

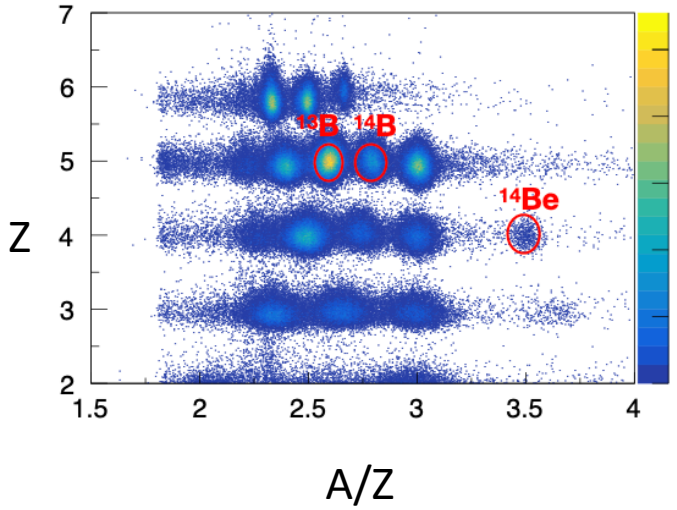

Mean-field + SRC simulation Doesn't Describe Data Well in bound ^{14}B channel

Data-driven methods required for ^{16}C SRC analysis

Selections

- (p,2p) tagging
- ^{14}B fragment tagging
- $|t|,|u| > 0.8$ GeV²
- $0.3 < M^2_{miss} < 1.5$ GeV²/c⁴
- $p_{miss} > 0.4$ GeV/c

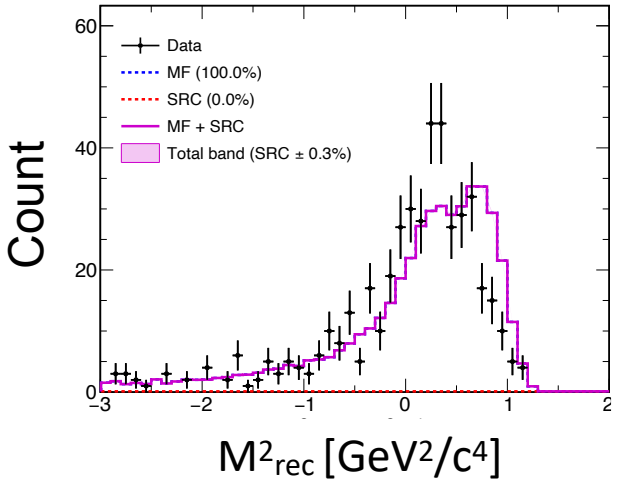

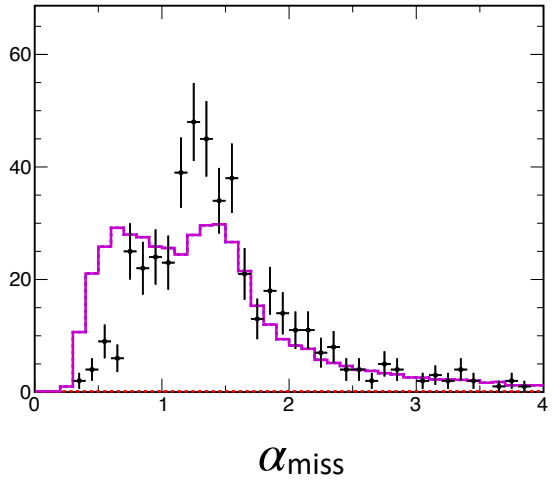

Bound ^{14}B channel data
NOT Consistent with ^{12}C pn-SRC Result

Inconsistency with SRC data in ^{12}C shows strong SRC suppression in bound ^{14}B channel

Selections

- (p,2p) tagging
- ^{14}B fragment tagging
- $|t|,|u| > 0.8$ GeV²
- $0.3 < M^2_{miss} < 1.5$ GeV²/c⁴
- $p_{miss} > 0.4$ GeV/c

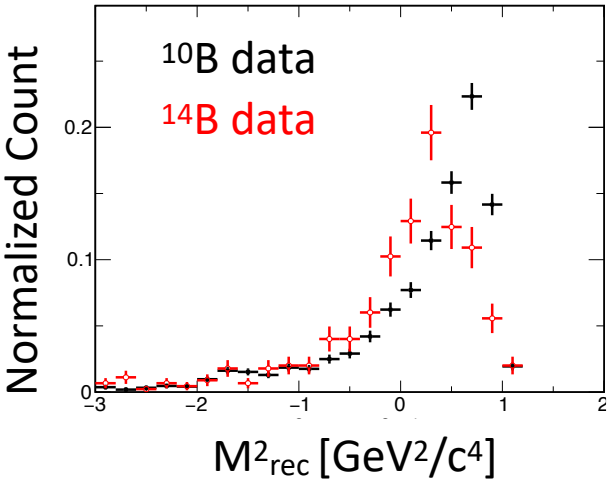

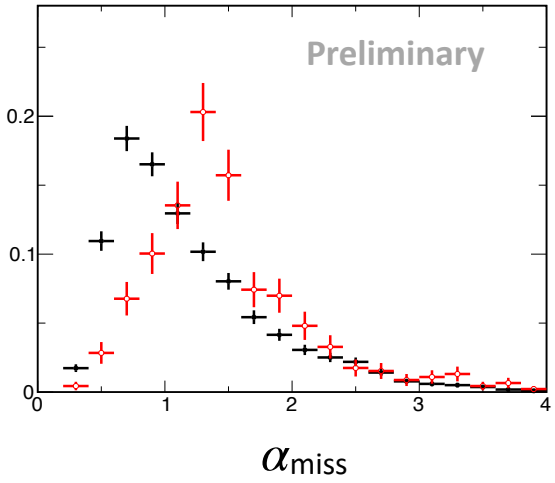

Bound ^{14}B channel data
Consistent with Mean-Field channel data

Consistency with mean-field data in ^{12}C(p,2p)^{11}B and ^{16}C(p,2p)^{15}B shows strong SRC suppression in bound ^{14}B channel

Selections

- (p,2p) tagging
- ^{14}B fragment tagging
- $|t|,|u| > 0.8$ GeV²
- $0.3 < M^2_{miss} < 1.5$ GeV²/c⁴
- $p_{miss} > 0.4$ GeV/c

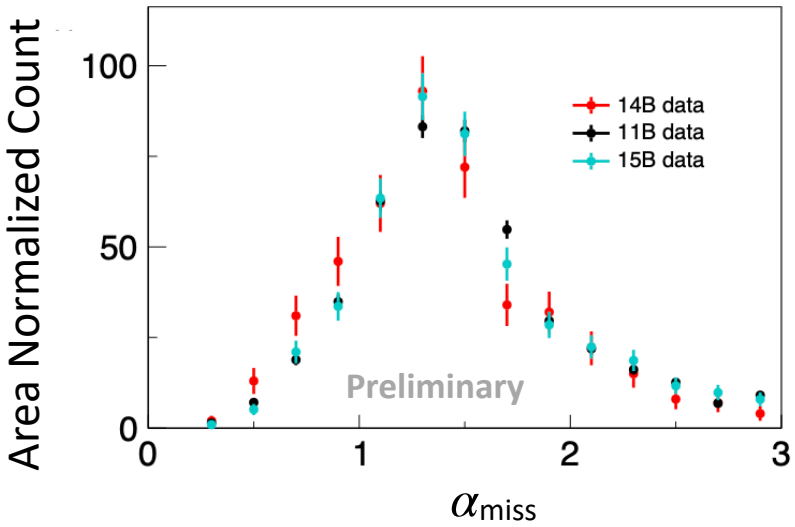

SRC Final-State Selectivity

No bound ^{14}B states available after deuteron-like pn-SRC pair removal

SRC pn pair ~ deuteron: T=0; $J^{\pi} = 1^{+}$

^{16}C - pn-SRC -> ^{14}B

$J^{\pi}=0^{+}$ - $J^{\pi}=1^{+}$ -> $J^{\pi}=1^{+}$

SRC Final-State Selectivity

No bound ^{14}B states available after deuteron-like pn-SRC pair removal

No known bound states with positive parity

E [MeV]	Jpi
0.0	2^-
0.74	(1^-)

SRC pn pair ~ deuteron: T=0; $J^\pi = 1^+$

^{16}C - pn-SRC -> ^{14}B

$J^\pi=0^+$ - $J^\pi=1^+$ -> $J^\pi=1^+$

SRC Final-State Selectivity

No bound ^{14}B states available after deuteron-like pn-SRC pair removal

No known bound states with positive parity

E [MeV]	Jpi
0.0	2^-
0.74	(1^-)

SRC pn pair ~ deuteron: T=0; $J^\pi = 1^+$

^{16}C - pn-SRC -> ^{14}B

$J^\pi=0^+$ - $J^\pi=1^+$ -> $J^\pi=1^+$

Bound ^{14}Be ground state available after pp-SRC pair removal

Bound ground state with positive parity

E [MeV]	Jpi
0.0	0^+

SRC pp pair: T=1; $J^\pi = 0^+$

^{16}C - pp-SRC -> ^{14}Be

$J^\pi=0^+$ - $J^\pi=0^+$ -> $J^\pi=0^+$

Bound ^{14}Be channel data *Consistent* with ^{12}C pp-SRC Result

Consistency with pp-SRC signal in ^{12}C suggests SRC presence in bound ^{14}Be channel
Consistent with quantum number arguments

Selections

- (p,2p) tagging
- A-2 fragment tagging
- |t|,|u| > 0.8 GeV²
- $0.3 < M^2_{miss} < 1.5$ GeV²/c⁴
- $p_{miss} > 0.4$ GeV/c

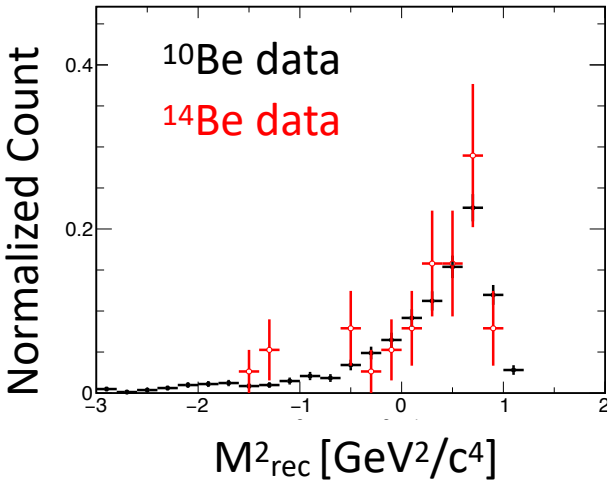

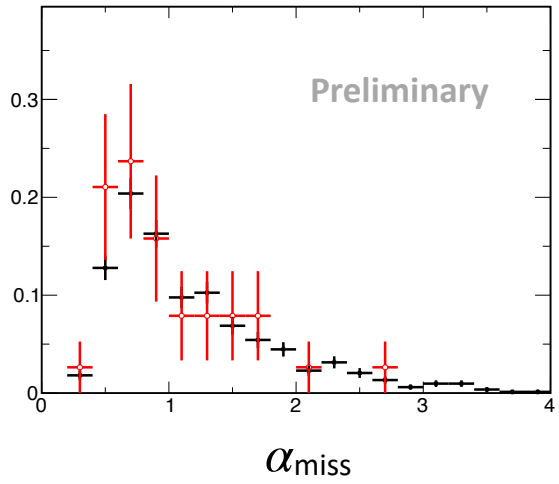

Limited statistics due to only 34% ^{14}Be fragment acceptance and low proton separation energy threshold.

Bound ^{14}Be channel data
Consistent with GCF simulation

Selections

- (p,2p) tagging
- ^{14}Be fragment tagging
- |t|,|u| > 0.8 GeV²
- $0.3 < M^2_{miss} < 1.5$ GeV²/c⁴
- $p_{miss} > 0.4$ GeV/c
- $\alpha_{miss} < 1.2$

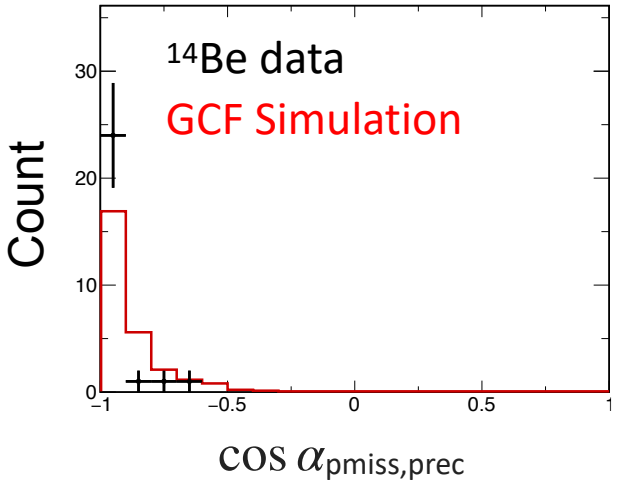

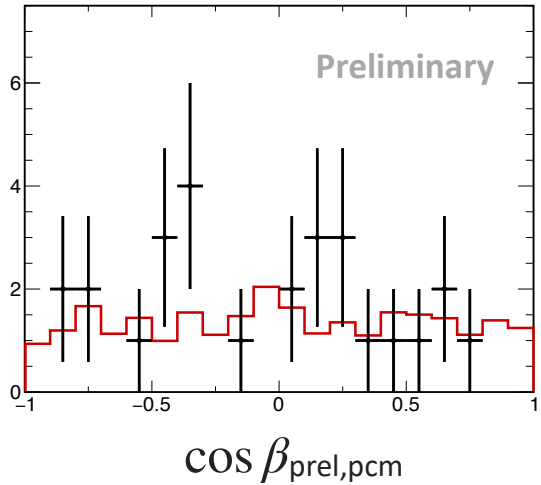

Unbound ^{14}B Channel (^{14}B* -> ^{13}B + n) *Consistent* with ^{12}C pn-SRC Results

Consistency with pp-SRC signal in ^{12}C suggests SRC presence in unbound ^{14}B* channel

Selections

- (p,2p) tagging
- A-2 fragment tagging
- |t|,|u| > 0.8 GeV²
- $0.3 < M^2_{miss} < 1.5$ GeV²/c⁴
- $p_{miss} > 0.4$ GeV/c

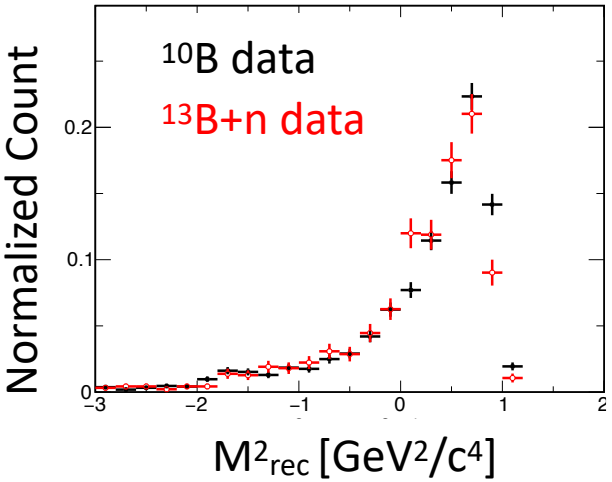

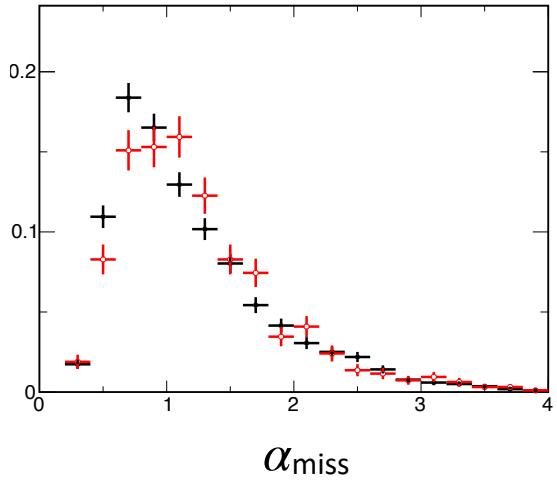

Evaporated nucleon within GLAD magnet acceptance. See backup slides.

Conclusions

SRC identification in 12C with significant statistics

- SRC signals in proton-probe experiment consistent with electron-probe results
- pn-SRC data in 12C favors realistic AV18 potential over unrealistic AV4’ potential

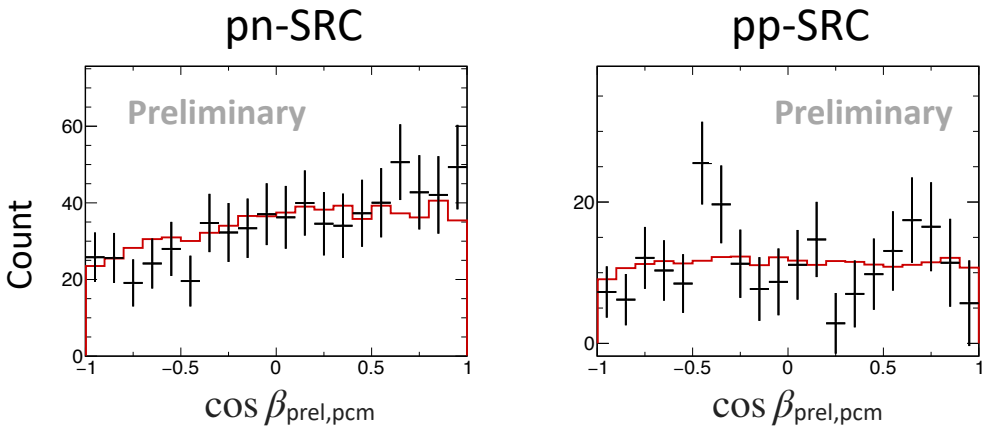

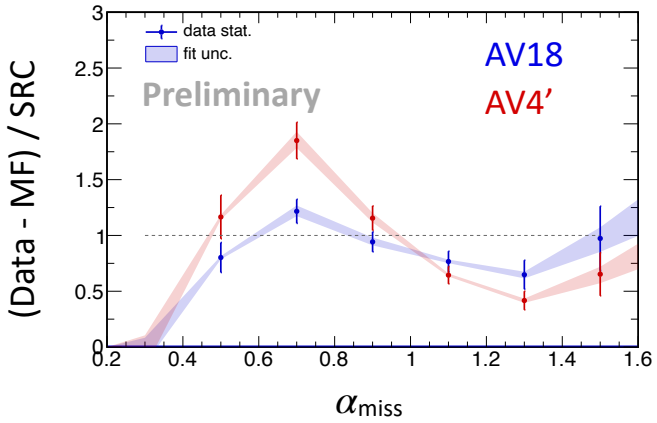

Conclusions

First measurement of SRC in radioactive nuclei

- SRC signals in ^{16}C suggested in ^{14}Be, ^{14}B*(^{13}Bn) channels through data-driven method
- SRC suppression in bound ^{14}B channel suggests quantum number selectivity

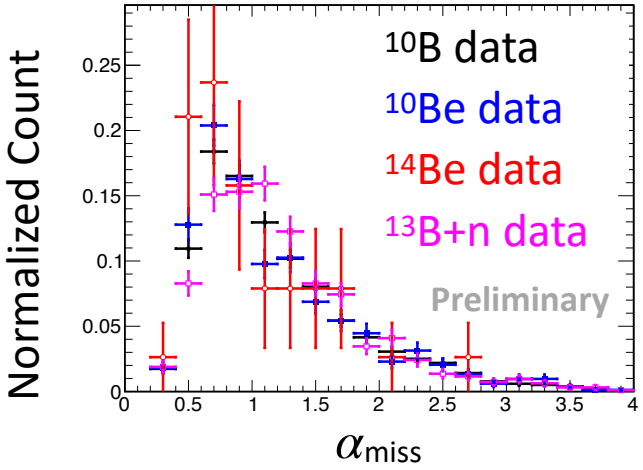

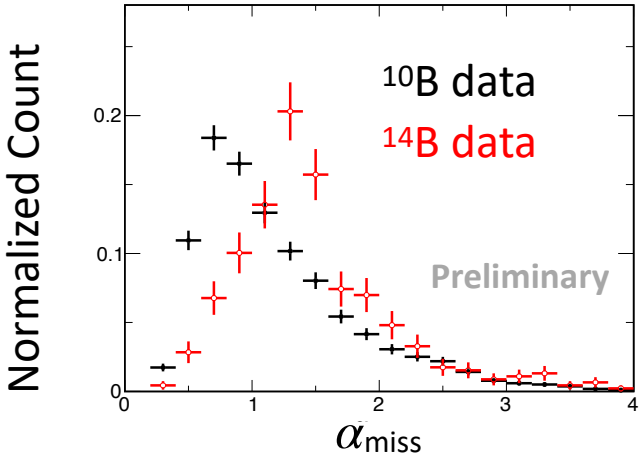

Thank you!

Backup slides

SRC pn / pp ratio

- pn-SRC in $^{12}C(p,2p)^{10}B$: 1327 * (51.8 ± 4.1%) = 687.4 ± 54.4
- pp-SRC in $^{12}C(p,2p)^{10}Be$: 506 * (44.8 +/- 7.1%) = 226.7 ± 36.0
- pn-SRC in ^{10}B / pp-SRC in ^{10}Be = 3.0 +/- 0.5
- Single charge exchange (SCE): $^{10}B(p,n')^{10}Be$; $^{10}Be(n,p')^{10}B$
- 2% SCE: pn-SRC in ^{10}B / pp-SRC in ^{10}Be = 3.2 +/- 0.6
- 8% SCE: pn-SRC in ^{10}B / pp-SRC in ^{10}Be = 4.0 +/- 1.0

SRC pn / pp ratio

- pn-SRC in $^{12}C(p,2p)^{10}B$: 1327 * (51.8 ± 4.1%) = 687.4 ± 54.4
- pp-SRC in $^{12}C(p,2p)^{10}Be$: 506 * (44.8 ± 7.1%) = 226.7 +/- 36.0
- pn-SRC in ^{10}B / pp-SRC in ^{10}Be = 3.0 +/- 0.5
- Single charge exchange (SCE): $^{10}B(p,n')^{10}Be$; $^{10}Be(n,p')^{10}B$
- 2% SCE: pn-SRC in ^{10}B / pp-SRC in ^{10}Be = 3.2 +/- 0.6
- 8% SCE: pn-SRC in ^{10}B / pp-SRC in ^{10}Be = 4.0 +/- 1.0
- Final state selectivity affects the pn- / pp-SRC ratio

INCL describes mean-field $^{12}C(p,2p)^{11}B$ channel

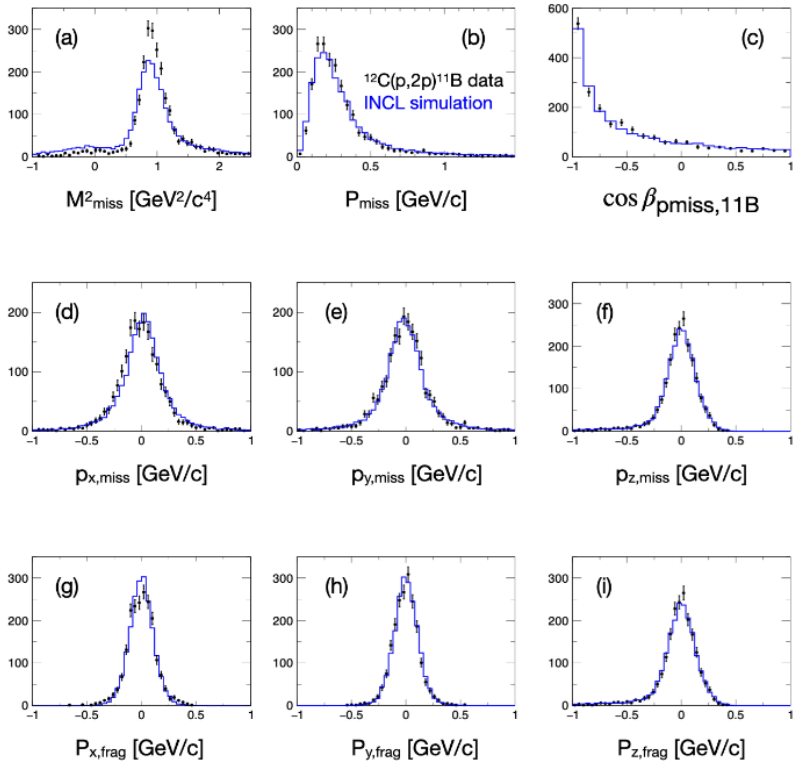

Kinematic fitting for ^{10}B channel

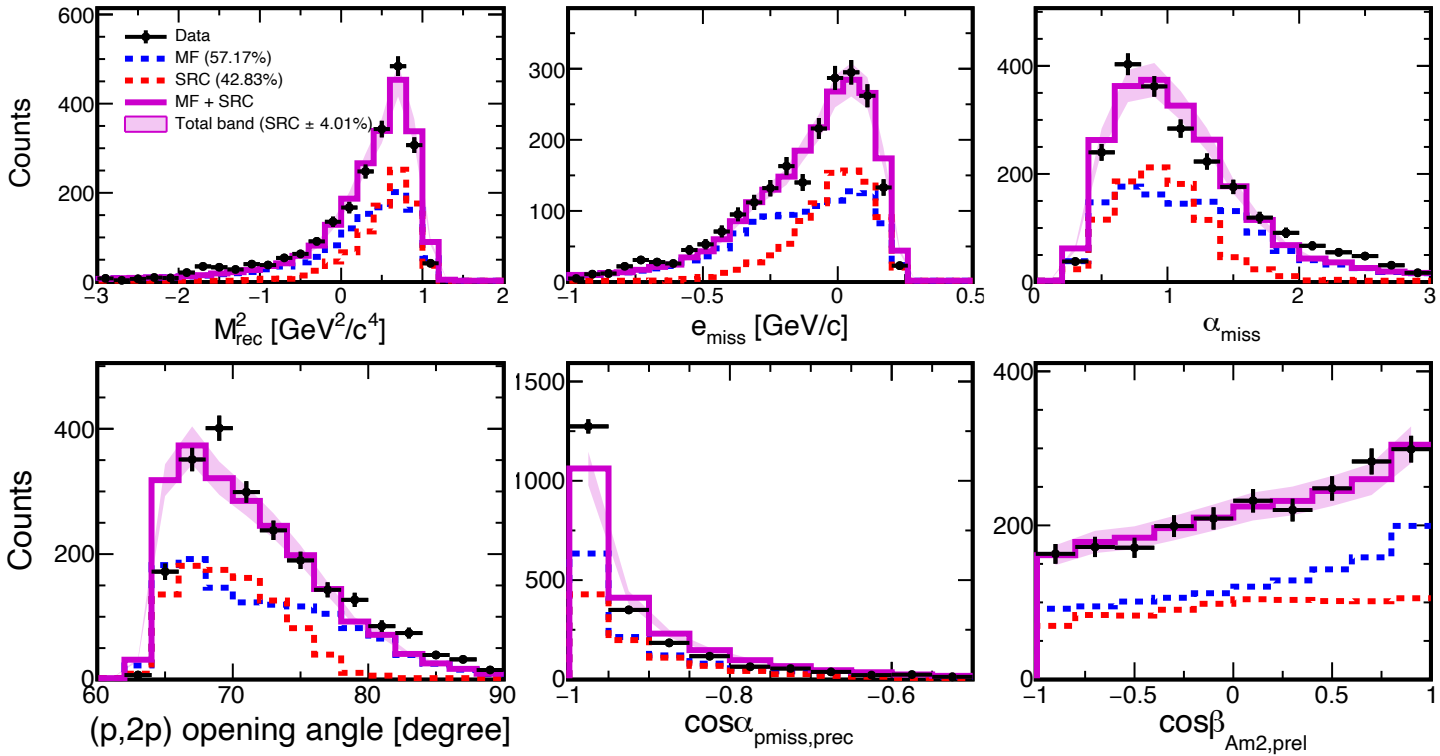

Kinematic fitting for ^{10}Be channel

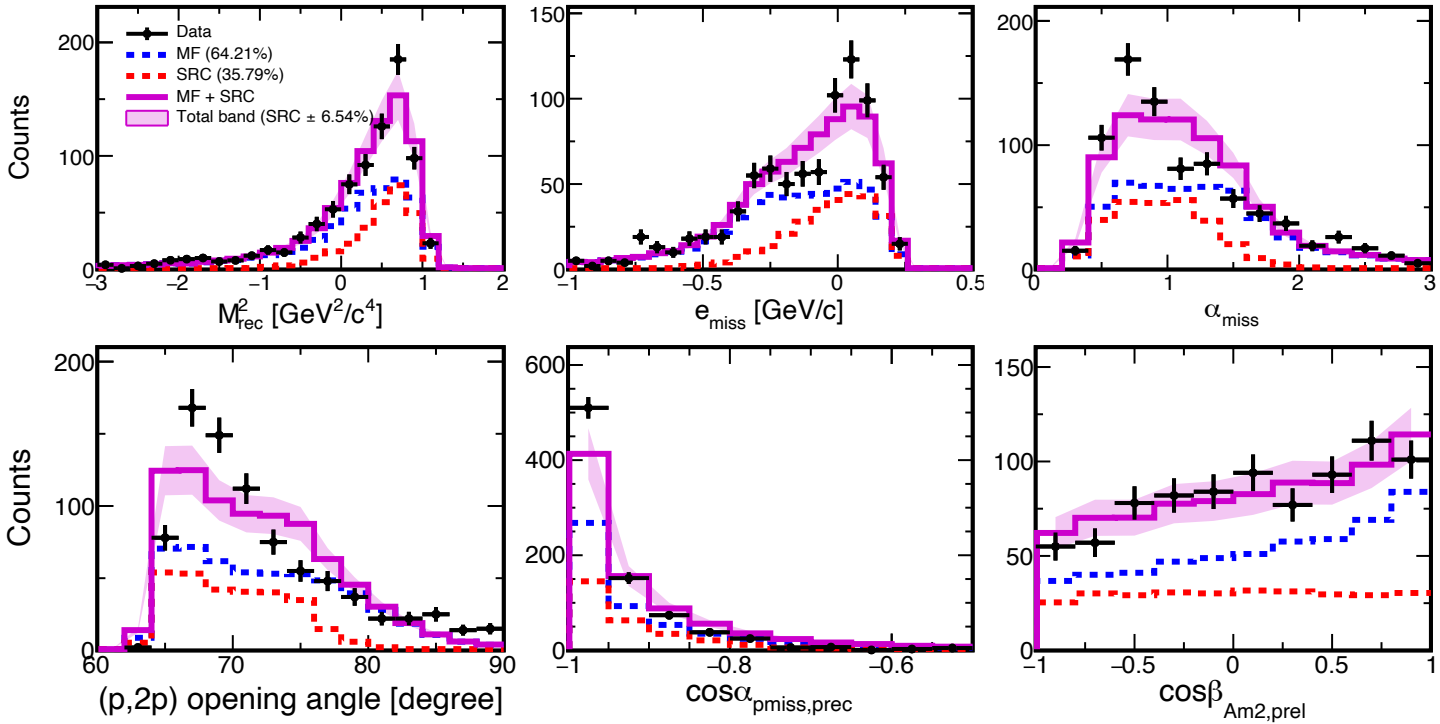

Kinematic fitting for ^{14}B channel

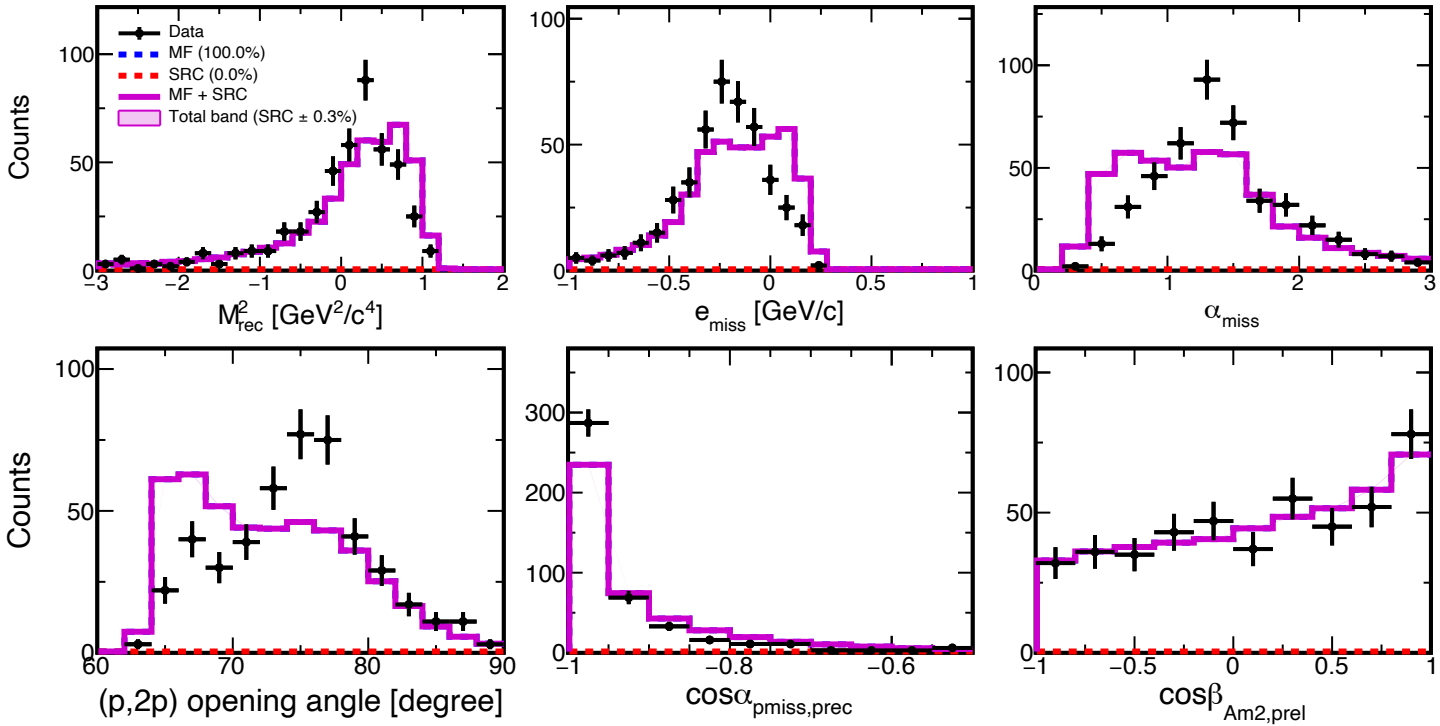

Kinematic fitting for ^{14}Be channel

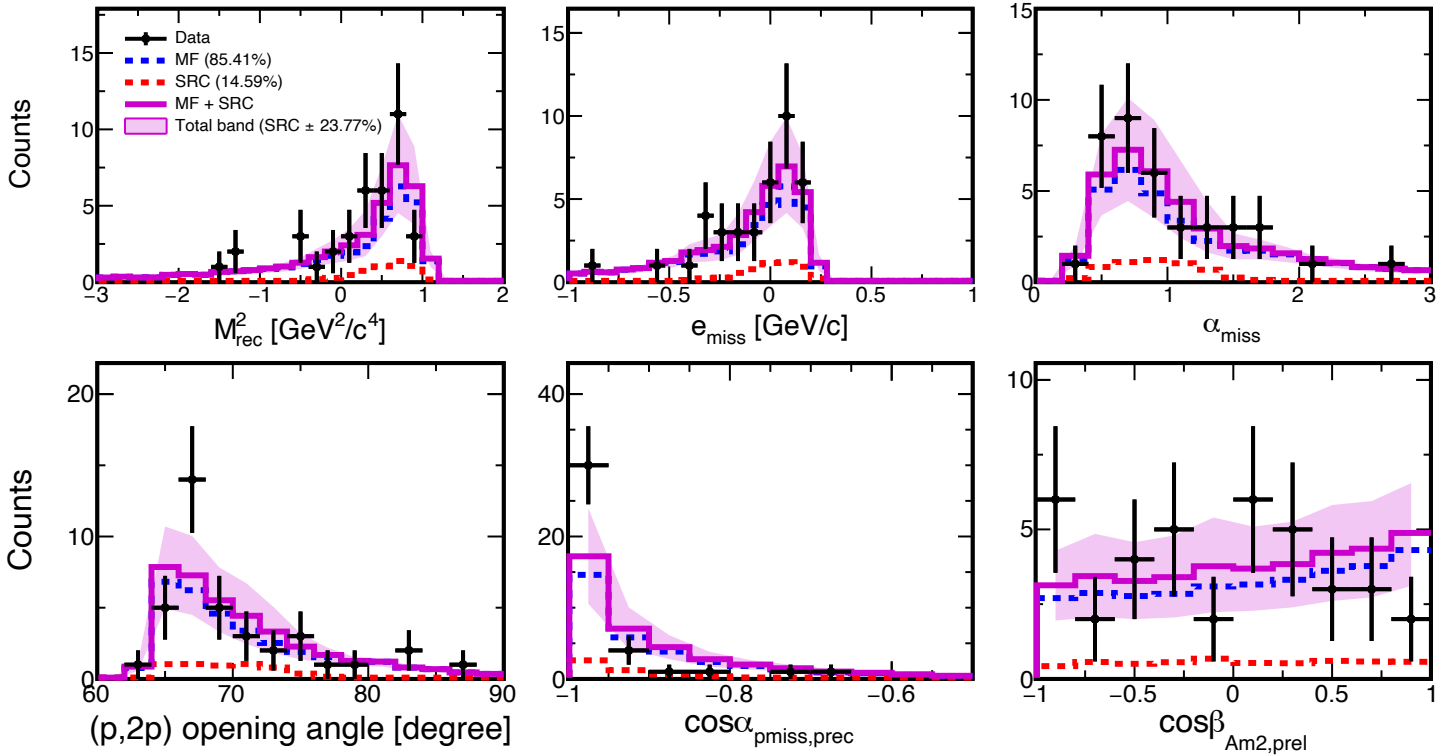

Kinematic fitting for ^{13}B+n channel

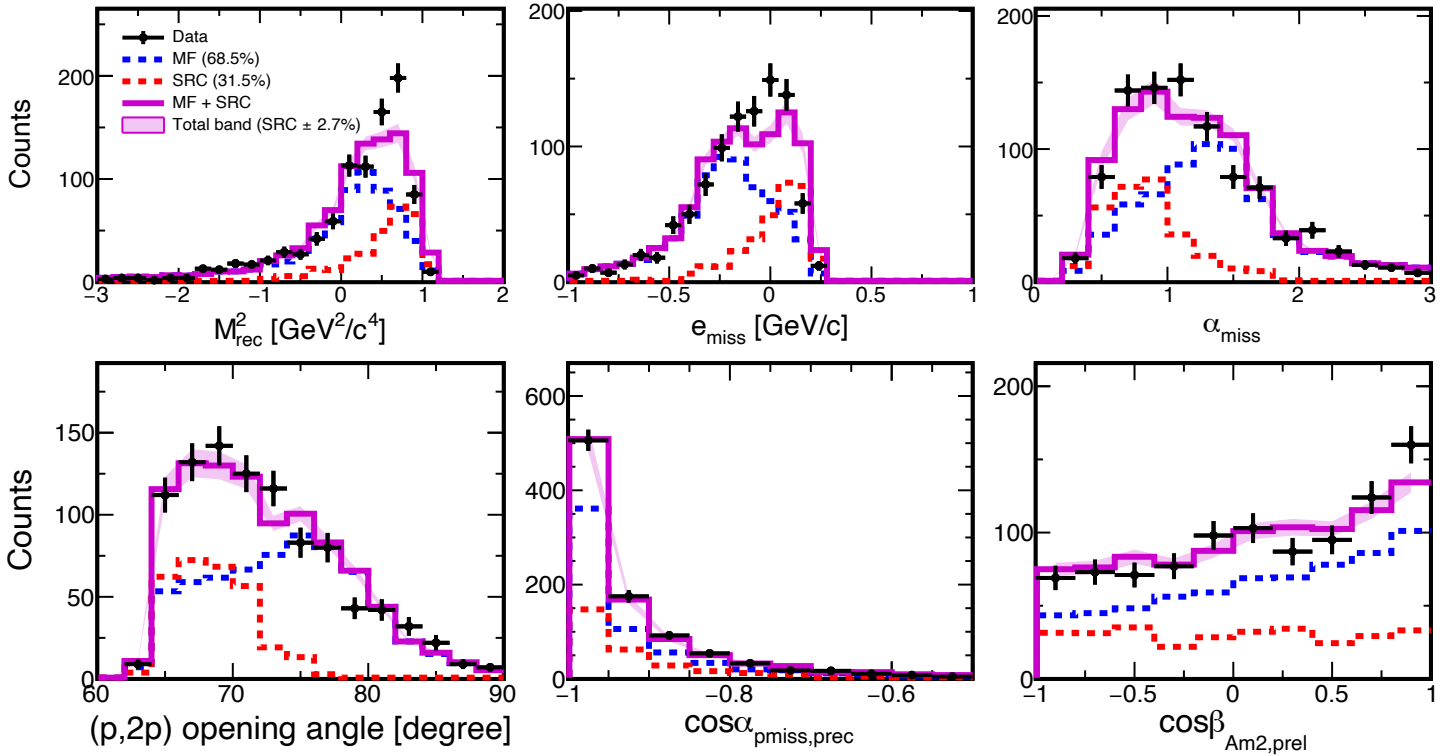

$^{14}B^{*}->^{13}B+n$ neutron acceptance

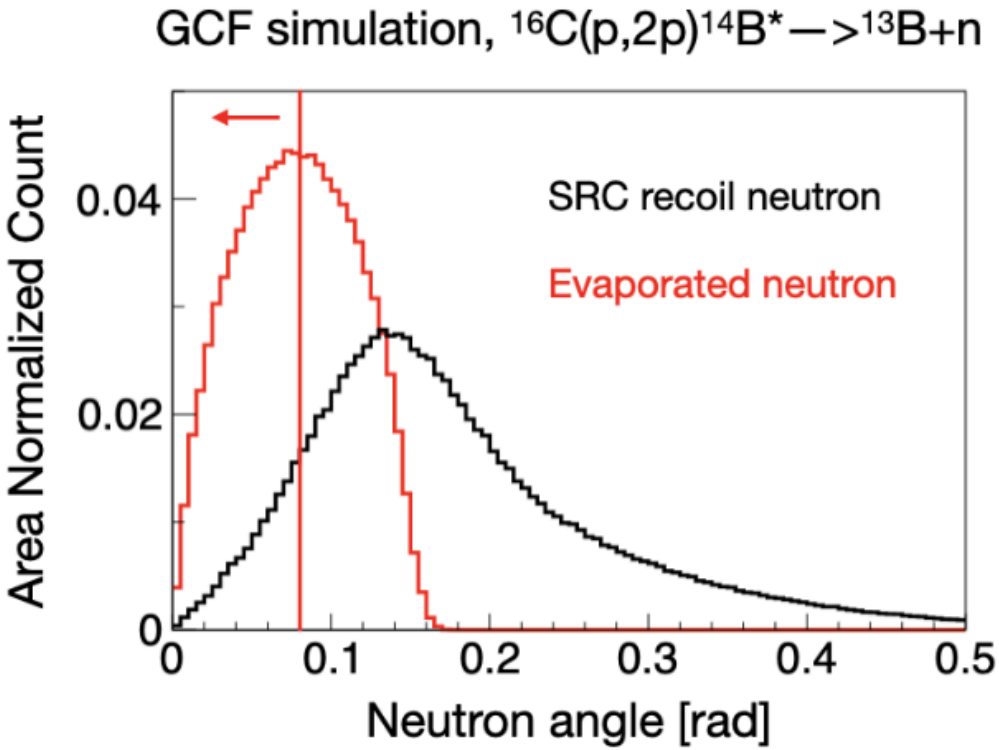

R³B Setup

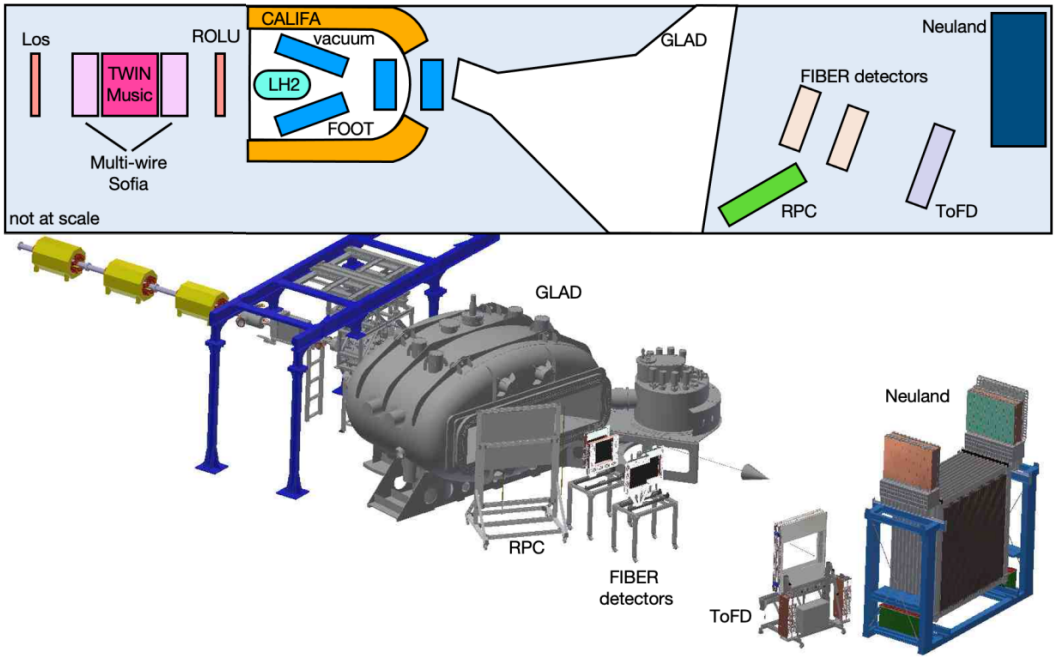
Los
ROLU
CALIFA
vacuum
LH2
FOOT
TWIN
Music
Multi-wire
Sofia
not at scale
GLAD
Neuland
FIBER detectors
RPC
ToFD
GLAD
Neuland
RPC
FIBER
detectors
ToFD

R³B Setup

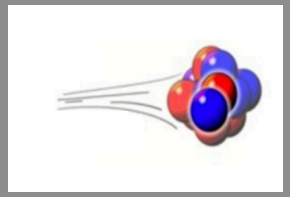

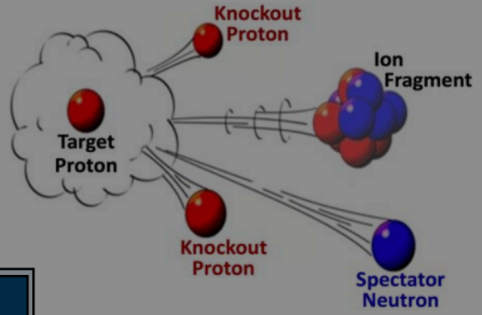

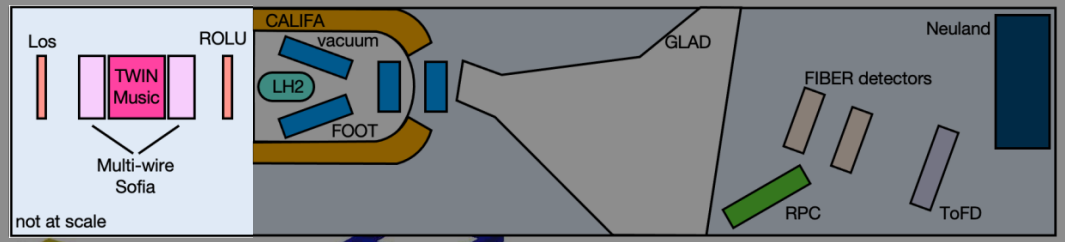

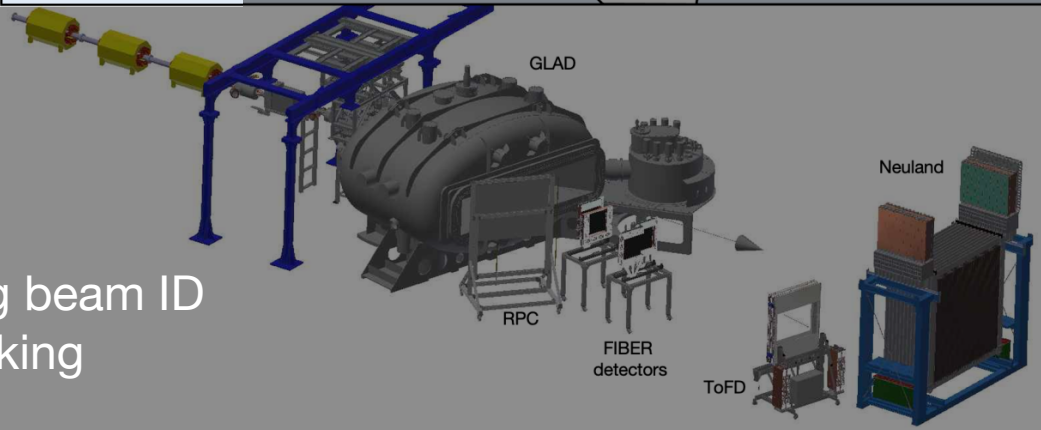

Incoming beam ID
And tracking

R³B Setup

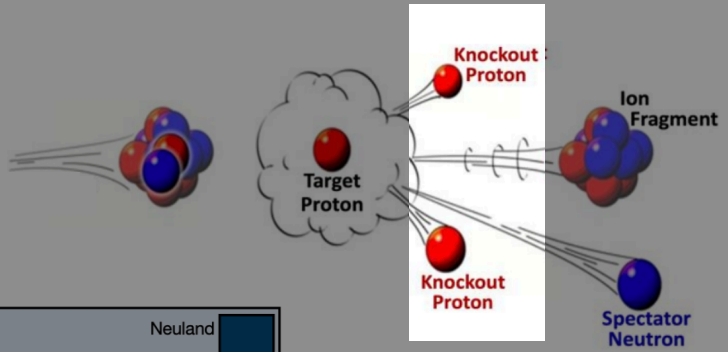

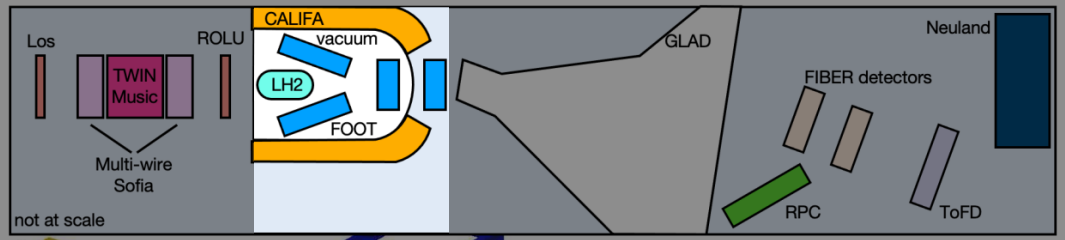

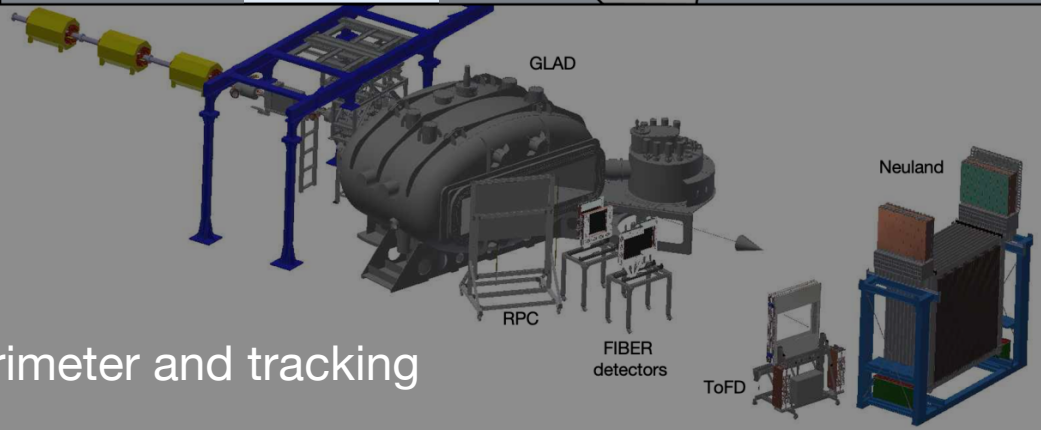

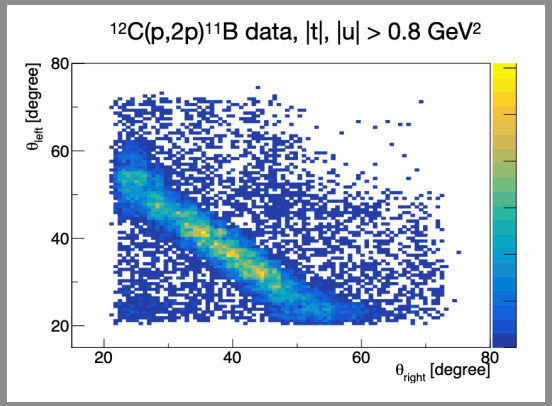

p,2p calorimeter and tracking

R³B Setup

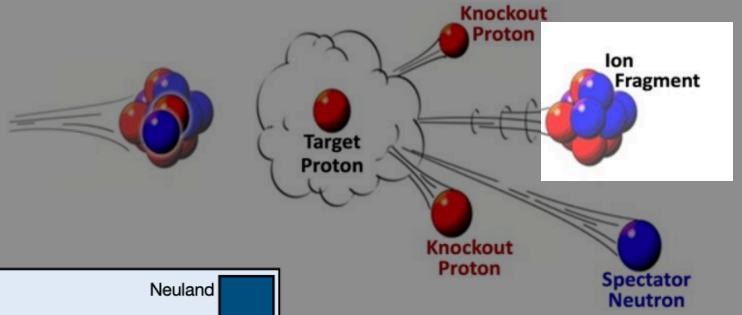

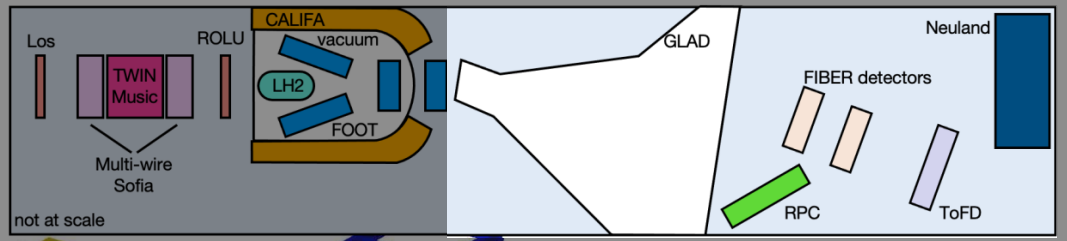

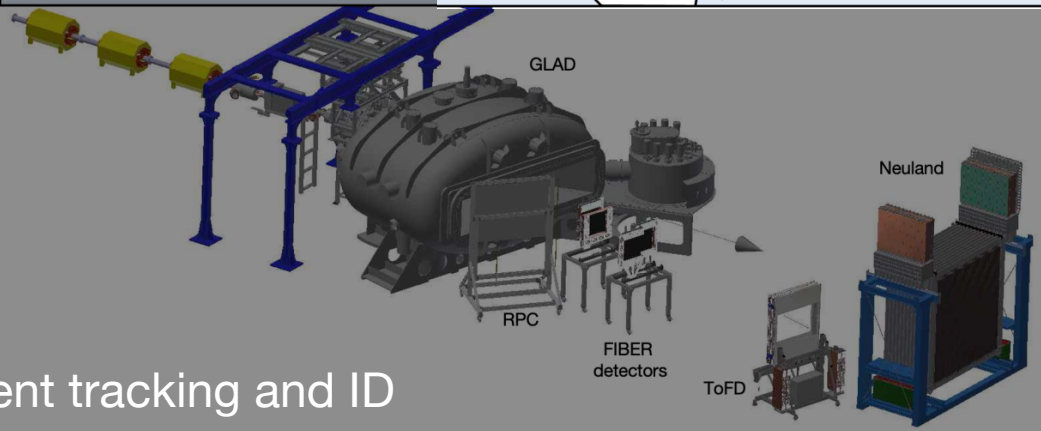

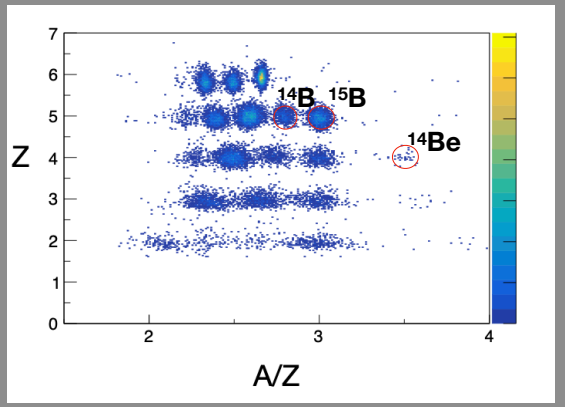

Fragment tracking and ID